J Polym Res (2013) 20:42
DOI 10.1007/s10965-012-0042-z

ORIGINAL PAPER

Study on the self-assembly properties of fluorinated hydrophobically associating polyacrylamide

Chen Wang · Xiaorui Li · Biao Du · Yiding Shen · Peizhi Li

Received: 30 August 2012 / Accepted: 28 November 2012 / Published online: 27 December 2012

Abstract The self-assembly of a fluorinated hydrophobically associating polyacrylamide (UFPAM) prepared by emulsifier-free ultrasound-assisted radical polymerization was studied using fluorescence spectroscopy (FS), rheological measurements, and dynamic light scattering (DLS). The effects of the degree of mineralization (*M*), temperature, and the concentrations of ionic surfactants—sodium dodecyl sulfate (SDS) and cetyltrimethyl ammonium bromide (CTAB)—on the self-assembly behavior of UFPAM were explored in detail. The results showed that 2,2,3,4,4,4-hexafluorobutyl methacrylate (FA) was effectively incorporated into the UFPAM. As the concentration of UFPAM increased, the hydrophobic self-assembly behavior of UFPAM increased the apparent viscosity and enhanced the structural network of UFPAM, as indicated by the Ostwald–de Waele power-law model, FS, dynamic rheological measurements, and DLS. The maximum apparent viscosity of the UFPAM solution occurred when the polarity of the solution was enhanced in mineralized solution and the polymer coils were expanded at increased temperature. Provided that the concentration of the ionic surfactant was below its CMC, the addition of CTAB promoted the self-assembly of UFPAM, but this did not occur upon the addition of SDS. When the concentration of the surfactant was above the CMC, the aggregation number increased in the UFPAM–CTAB system, whereas it exhibited a minimum value in the UFPAM–SDS system.

C. Wang (✉) · X. Li · Y. Shen · P. Li
Key Laboratory of Auxiliary Chemistry & Technology for Chemical Industry, Ministry of Education, Shaanxi University of Science & Technology,
Xi'an 710021, People's Republic of China
e-mail: 277365553@qq.com

B. Du
Chemical Corporation of Changqing,
Xi'an 710021, People's Republic of China

Keywords Hydrophobically associating polyacrylamide · Self-assembly behavior · Ultrasound assisted · Fluorocarbon monomer · Aggregation number · Hydrophobic microdomain

Introduction

Over the past two decades, hydrophobically associating polyacrylamides (HAPAMs), which consist of a hydrophilic polyacrylamide backbone (the major component) and hydrophobic groups (the minor component) [1–3], have attracted considerable attention due to their outstanding solution properties and numerous practical applications [4–9]. These polymers exhibit a strong tendency to self-associate via intra- or interpolymer interactions among the hydrophobic side chains.

Recently, many kinds of hydrophobically associating polyacrylamides have been prepared using different hydrophobic monomers or different synthetic pathways [10, 11]. So far, most of these studies have concentrated on modifying the water-soluble polymer with hydrophobic hydrocarbon chains [4]. On the other hand, fluorocarbon chains have lower surface energies and a stronger tendency to associate than hydrocarbon chains [12]. Thus, HAPAMs synthesized using fluorocarbon chains have superior thickening properties, salt resistance, and heat resistance compared to those produced using hydrocarbon chains.

HAPAMs are usually synthesized using micellar copolymerization [13, 14]. However, many researchers have found that ultrasonic waves aid dispersion and radical polymerization initiation (i.e., ultrasound-assisted radical polymerization) through acoustic cavitation [15, 16], obviating the need for a surfactant. So far, only a few works on the synthesis of hydrophobically associating polyacrylamides via emulsifier-free ultrasound-assisted radical polymerization have been published, and such an approach to the synthesis of

modified hydrophobically associating polyacrylamides with fluorinated monomers has barely been addressed.

Therefore, as described in the remainder of this paper, we examined a fluorinated hydrophobically associating polyacrylamide (UFPAM) that was successfully prepared by emulsifier-free ultrasound-assisted radical polymerization. Fluorescence spectroscopy, rheological measurements, and dynamic light scattering were used to study the self-assembly of UFPAM in solution as well as the effects of the degree of mineralization, the temperature, and the concentrations of ionic surfactants on this self-assembly behavior.

Experimental

Materials

Acrylamide (AM) was purchased from Tianjin Kermel Chemical Reagent Co., Ltd. (Tianjin, China). 2,2,3,4,4,4-Hexafluorobutyl methacrylate (FA) was purchased from Harbin Xeogia Group Co., Ltd. (Harbin, China). 2-Acrylamido-2-methyl propane sulfonic acid (AMPS) was from Zhonghai Chemical Industry (Shandong, China). 2,2′-Azobis(2-amidinopropane) dihydrochloride (AIBA V-50) was purchased from Tianjing Hongyan Chemical Reagent Co., Ltd. (Tianjin, China). Diphenyl ketone and pyrene were obtained from Fluka (Buchs, Switzerland), and the pyrene was recrystallized three times from absolute ethanol.

All chemicals were of analytical grade and were used as received without further purification (except for pyrene). Distilled water was used in all experiments.

A KQ-300VDE (Kunshan Ultrasonic Apparatus Co., Ltd., Shanghai, China) double-frequency ultrasonic tank was used.

Synthesis of UFPAM

Specific amounts of AM, AMPS, and FA as well as an appropriate amount of deionized water were added to a 250 ml beaker and mixed by high-speed mechanical stirring. The mixture was adjusted with NaOH to pH=9.5 and purged with nitrogen for at least 10 min. The beaker was then placed in an ultrasonic tank in which the water was kept at 50 °C. The AIBA solution was injected into the reaction mixture, and the resultant mixture was allowed to react continuously for 1 h. The product (UFPAM) was gelatiniform and clear. It was dried directly under vacuum at 50 °C for 12 h and finally broken down into powder. (The need to use a complicated process to remove the surfactant used in micellar polymerization was thus avoided [17].) The conditions of the synthesis were as follows: *w*(AM):*w*(AMPS):*w*(FA)= 85:13:2, the total monomer concentration was 10 g/dL, and the AIBA concentration was 0.3 wt% based on the total monomer weight. The AMPS monomer was converted into salt form before polymerization (at pH9.5, which was achieved through the addition of concentrated NaOH). The water temperature in the ultrasonic tank was maintained at 50 °C. The ultrasonic power employed was 140 W.

Preparation of standard mineralized water

The degree of mineralization (*M*) is defined as the number of milligrams of salt (of all kinds) in 1 L of water. Standard mineralized water was prepared as follows. 4902.68 g of distilled water was added to a 10 L beaker that was continuously stirred in order to form a vortex by vigorous mechanical working. 5.7165 g of anhydrous calcium chloride, 4.3150 g of magnesium chloride hexahydrate, and 87.2890 g of sodium chloride were then added slowly in order. (Each was completely dissolved before adding the next.) The *M* value for this solution was 19,334 mg/L. The total concentrations of calcium and magnesium ion were 514 mg/L. Other mineralized waters were prepared by increasing or decreasing the salt concentrations accordingly. The final *M* was determined by a method described in the *The Industry Standard of the People's Republic of China—Determination of Mineralized Degree (Gravimetric Method)*.

Measurements

Infrared spectroscopy of the FSM was carried out using a model V70 FT-IR from Bruker (Rheinstetten, Germany).

^{19}F NMR spectra were recorded on a Bruker DPX-400 spectrometer at 376.3 MHz at a digital resolution of± 0.01 ppm, with 0.05 % in D_2O used as solvent.

The viscosities and other external parameters as well as the rheological behaviors of the sample solutions were measured using a HAAKE RS6000 electro-rheometer (Thermo Fisher Scientific, Waltham, MA, USA).

Multiangle DLS measurements were carried out on the samples at five different scattering angles (50, 70, 90, 110, and 130°) using a model 4800 photon correlation spectrometer from Malvern Instruments (Malvern, UK). The samples were precipitated into a large amount of ethanol, and the sample solutions were filtered through a 450 nm Durapore membrane (Millipore, Billerica, MA, USA) before testing.

The fluorescence spectroscopy (FS) measurements were performed with a Cary Eclipse fluorophotometer (Varian, Palo Alto, CA, USA) at 25 °C with excitation at 338 nm, a bandpass slit width of 3.0 nm, and a scanning range of 350–550 nm. Pyrene was used as the fluorescent probe. Solutions for fluorescence measurements were prepared by first pipetting 0.012 ml of a pyrene stock solution (2×10^{-4} mol/l in

ethanol) into a flask. Then, 3 ml of polymer solution with a given concentration were added to the flask and ultrasound was applied for 0.5 h before the FS measurements were carried out [18]. Diphenyl ketone was used as the quencher. The micellar aggregation number N was deduced using the following equation [19]:

$$\ln I = \ln I_0 - \frac{N[\mathrm{Q}]}{[S] - CMC} \quad (1)$$

where [Q] and [S] are the concentrations of quencher and total surfactant, respectively. I_0 and I are the fluorescent intensities at 371 nm in the absence and presence of the quencher.

Results and discussion

Characterization of UFPAM

FT-IR

The FT-IR spectra of FA and UFPAM are shown in Fig. 1. These have wide absorption bands at 3,300~3,500 cm^{-1} due to N–H stretching vibrations, which may derive from the formation of strong hydrogen bonds among polymer molecules or among polymer molecules and water molecules. Also, since this polymer shows high water absorbency, combining the polymer with a small amount of water leads to a wide band due to O–H stretching vibrations at >3,000 cm^{-1}, which is actually due to the overlap of two absorption bands. The characteristic stretching vibrations of C=O in acrylamide appear at 1,669 cm^{-1}. The absorption bands at 1,192 and 1,042 cm^{-1} correspond to symmetric and asymmetric stretching vibrations of the SO_3 in AMPS. The band at 1,730 cm^{-1} is due to stretching vibrations of C=O in the ester FA, whereas stretching vibrations of C–F produce peaks at 1,307 and 1,188 cm^{-1} [20].

The above data include all of the characteristic absorptions of the functional groups in AM, AMPS, and FA, and demonstrate that FA was effectively introduced into UFPAM by emulsifier-free ultrasound-assisted radical polymerization.

^{19}F-NMR

As shown in the ^{19}F NMR spectrum (Fig. 2), there are three different chemical environments of the fluorine atoms in UFPAM. Due to the effects of van der Waals forces and coupling, double peaks from the $-CF_3$ groups appear in the low-field range (near −67.79 ppm), while peaks from the $-CF_2$ groups appear at around −110.19 ppm. Peaks from –CHF appear in the high-field range (−204.98 ppm), but do not show any influence of van der Waals forces [21]. These ^{19}F NMR results confirm that the FA was effectively introduced into UFPAM by emulsifier-free ultrasound-assisted radical polymerization.

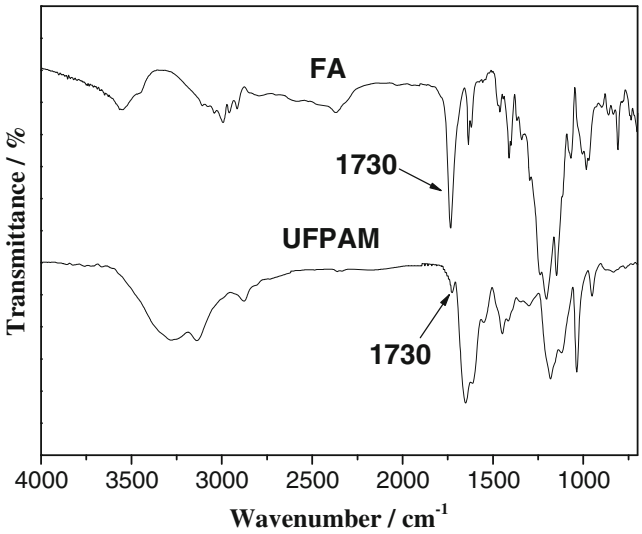

Fig. 1 FT-IR spectra of FA and UFPAM

Power-law model of the self-assembly behavior of UFPAM

It was proposed that a power-law model could accurately reflect the rheological properties of the solution. The relationship between lgσ and lgγ for aqueous solutions of UFPAM, as shown in Fig. 3, correlated perfectly with the following Ostwald–de Waele power-law model (the regression coefficients were all above 0.9970, as shown in Table 1) [22]:

$$\eta_a = k \cdot \gamma^{n-1} \quad \text{or} \quad \sigma = \mathrm{k} \cdot \gamma^{\mathrm{n}}, \quad (2)$$

where η_a is the apparent viscosity, σ is the shear stress, and γ is the shear rate. Taking logarithms of both sides of the equation above yields

$$\lg \sigma = \lg k + n \lg \gamma, \quad (3)$$

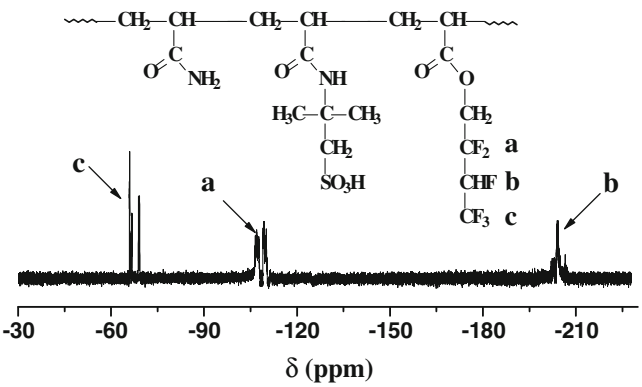

Fig. 2 ^{19}F NMR spectrum of UFPAM

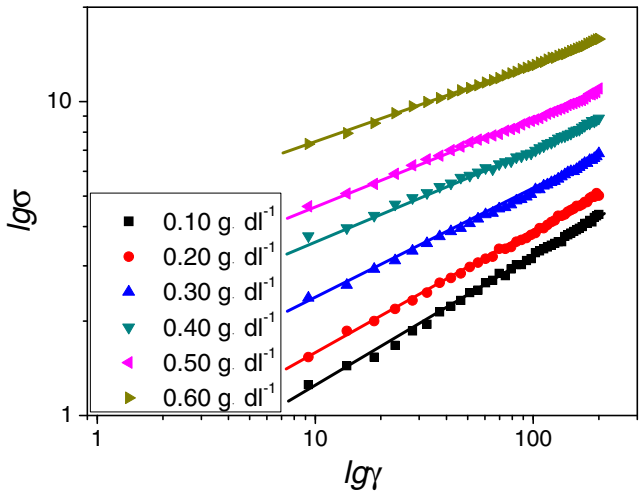

Fig. 3 The relationship of lgσ to lgγ for aqueous solutions of UFPAM

which was used in the present work to obtain n and k through linear regression. n is the liquidity index, which is 1 for a Newtonian fluid and <1 for a non-Newtonian fluid; k is the consistency coefficient (the higher the value of k, the greater the apparent viscosity of the system), which can also indicate the system's structural strength (in other words, the system is more likely to have a strong structure if the value of k is high; Table 1). The value of n was always less than 1, whatever the concentration of UFPAM, although n decreased with increasing UFPAM concentration, which indicates that the UFPAM solution became increasingly non-Newtonian with increasing UFPAM concentration. At the same time, the consistency coefficient k increased markedly with UFPAM concentration; when the UFPAM concentration increased from 0.10 to 0.60 g dL^{-1}, k rose from 0.466 to 4.116 mPa s^n. It was therefore concluded that hydrophobic groups in the polymer easily and spontaneously form intermolecular hydrophobic associations. This hydrophobic self-assembly behavior caused the apparent viscosity to increase and enhanced the structural network of UFPAM.

Table 1 The n and k values for various concentrations (c) of UFPAM in aqueous solution

c (UFPAM) (g dL^{-1})	n	k (mPa s^n)	Regression coefficient
0.10	0.422	0.466	0.9970
0.20	0.392	0.647	0.9972
0.30	0.348	1.050	0.9981
0.40	0.333	1.878	0.9988
0.50	0.276	2.474	0.9992
0.60	0.252	4.116	0.9992

Determination of the critical association concentration (CAC) of UFPAM

The CAC of UFPAM was determined as 0.31 g dL^{-1}, based on the change in the apparent viscosity of UFPAM solutions (Fig. 4) according to the literature [23]. The resultant trend indicates that it was the FA being successfully introduced into UFPAM that endows the special increasing pattern of apparent viscosity. This nonlinear sudden increase of apparent viscosity in UFPAM due to transferring from intramolecules to inter-molecules at/near the critical association concentration, which made the macromolecular chains crosslinking and the hydrodynamics volume enhanced. It was the so called critical association concentration (CAC). However, the change in the apparent viscosity of an UFPAM solution is a macroscopic manifestation of its hydrophobic associative properties, which can be probed at the molecular level using fluorometry. In the fluorescence spectrum, the value of I_1/I_3, i.e., the ratio of intensities of the first (I_1=371 nm) to the third (I_3=383 nm) emission peak of pyrene, was measured. This is the so-called polarity parameter, which is strongly dependent on the polarity around pyrene: the stronger the polarity of the microenvironment around pyrene, the higher the value of I_1/I_3 [24, 25]. For example, the value of I_1/I_3 is 1.87 when the pyrene is in pure water and 0.58 when it is in (nonpolar) cyclohexane.

As shown in Fig. 4, the value of I_1/I_3 initially declined slightly with increasing UFPAM concentration, which is due to the existence of a small number of intramolecular hydrophobic microdomains in the UFPAM solution. When c (UFPAM) was in the range 0.30–0.40 g dL^{-1}, the value of I_1/I_3 dropped sharply because the number of hydrophobic microdomains formed by the fluorocarbon chains in FA increased greatly, which drastically weakened the polarity of the microenvironment surrounding pyrene. Due to the limited solubility of pyrene in UFPAM solution [26], the value of I_1/I_3 stayed roughly constant above c(UFPAM)= 0.50 g dL^{-1}. This result confirms the CAC value determined on the basis of literature values.

Dynamic moduli (G' and G'')

We have seen that the modification of polyacrylamide with FA leads to a marked increase in the viscosity of the UFPAM solution. Similarly, the viscoelastic behavior should be strongly influenced by the self-assembly behavior (physical crosslinks among the hydrophobic groups in FA) of UFPAM. Measurements were therefore performed in the linear viscoelastic regime. Figure 5 describes the storage modulus (G') and the loss modulus (G'') of UFPAM with different concentrations of copolymer. Increasing the copolymer concentration clearly enhances both moduli and shifts the relaxation spectrum to lower frequencies [27]. For 0.30 and 0.40 g dL^{-1}

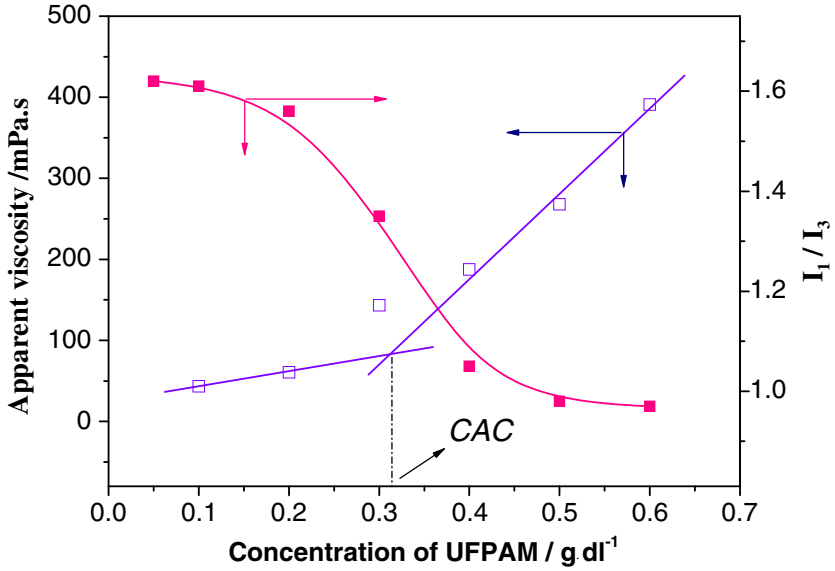

Fig. 4 Determination of the CAC for aqueous UFPAM. The apparent viscosity was determined for a shear rate of 7.6 s^{-1}

copolymer solutions, G' exceeded G'' at a certain frequency, which illustrates the importance of the elastic component of the UFPAM solution. The higher the copolymer concentration, the lower the frequency at which G' surpassed G''. In the case of Maxwellian behavior, a characteristic relaxation time τ_c can be estimated from the frequency ω_c corresponding to the crossing point G_c ($\tau_c=1/\omega_c$). The results showed that τ_c was less than 0.1 s in 0.10 g dL^{-1} copolymer solution, although this was not an exact result due to the limited frequency range. This parameter increased to approximately 1.0 s at 0.30 g dL^{-1} and 5.5 s at 0.40 g dL^{-1} copolymer solution. This obvious increase in τ_c with increasing copolymer concentration indicates that the structure of UFHAM contains more physical crosslinking and associations at higher concentrations, leading to enhanced viscoelasticity [28].

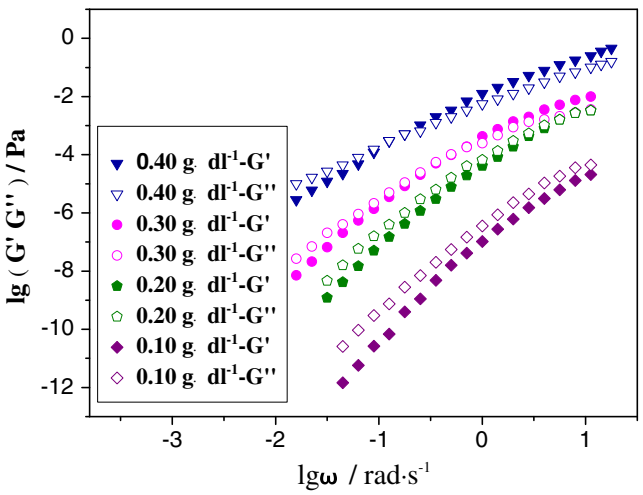

Fig. 5 Storage modulus (G') and loss modulus (G'')

Apparent aggregate size

Dynamic light scattering (DLS) is an effective method for studying the properties of hydrophobic polyacrylamide in aqueous solution [29], which reflect its self-assembly behavior in solution. Figure 6 shows how the apparent aggregate size distribution and the average apparent aggregate size (d*) change with increasing copolymer concentration. When the concentration of UFPAM was below the CAC (0.20 g dL^{-1}; curve (2) in Fig. 6), d* was approximately 839 nm, which is much larger than the pore diameter for the filter membrane (450 nm), demonstrating that associative behavior had already occurred by this stage. Obviously, the apparent aggregate size distribution shifts to a larger size with increasing UFPAM concentration, and changes from a monodispersion to a polydispersion. When the UFPAM concentration is higher than the CAC (0.40 g dL^{-1}), more large-sized

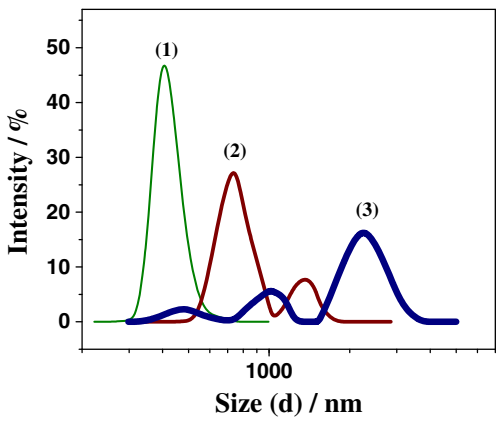

Fig. 6 Apparent aggregate sizes at different UFPAM concentrations: (*1*) 0.10 g dL^{-1}, d*=424 nm; (*2*) 0.20 g dL^{-1}, d*=839 nm; (*3*) 0.40 g dL^{-1}, d*=2,270 nm

aggregates are generated and d^* becomes 2,270 nm due to the hydrophobically associating effect changing from the mainly intra-molecules to the inter-molecules in aqueous solution. Therefore, crosslinked structures formed and each aggregate contained different numbers of UFPAM molecules.

Effect of shear rates on the self-assembly behavior of UFPAM

Figure 7 illustrates that the UFPAM solution exhibits shear thinning, which implies that it is a pseudoplastic fluid [30]. This behavior was clearly seen when the *c*(UFHPM) was near to or above the CAC, which was attributed to the emergence of intermolecular associative effects (physical crosslinking) in this regime. These self-assembled structures with physical crosslinks were broken under the application of shear force. However, when the copolymer concentration was below or near to the CAC, few associations occurred among the molecules, which led to a gradual decrease in the apparent velocity with increasing shear rate (i.e., "shear thinning").

Thixotropy is the change in a material's viscosity over time due to the application of shear stress, and is seen in many kinds of liquids that possess microstructures. Because thixotropy represents a temporary change in the microstructure of the system, the viscosity should recover to its normal value after a period of time. In a hydrophobic associating polyacrylamide solution, such changes in microstructure result from the competition between two driving forces: the flowing shear force, which can cause structural failure, and the self-assembly behavior of hydrophobic groups, which can promote the generation of structure among molecules [31]. Thixotropy was clearly exhibited by the UFPAM solution (Fig. 8). Three-dimensional network structures formed through hydrophobic self-assembly associations (physical crosslinking),

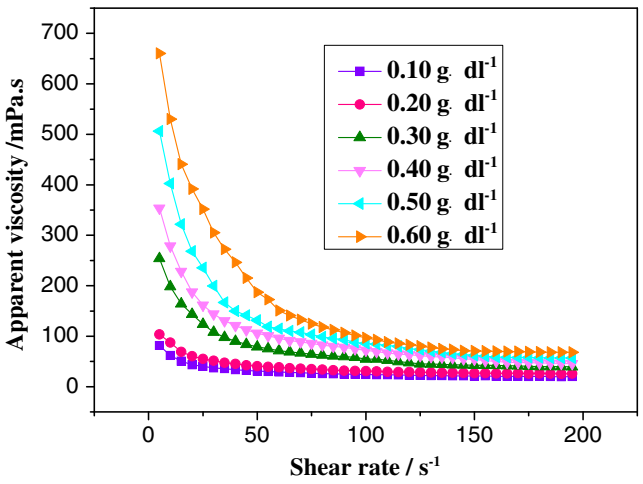

Fig. 7 Effect of shear rate on the apparent viscosity of UFPAM solution

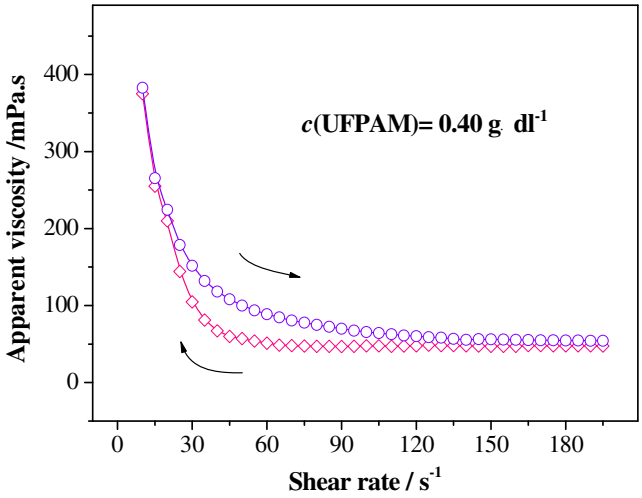

Fig. 8 Thixotropic behavior of UFPAM

which could be destroyed by applying shear force. Therefore, when the shear force was applied, the apparent viscosity declined, but when the shear force decreased or was removed, the network structure was regenerated in the system and the apparent viscosity recovered.

Self-assembly behavior of UFPAM in mineralized water

The self-assembly behavior of UFPAM in the mineralized water was studied by analyzing the relationship between the degree of mineralization (*M*) and the apparent viscosity of the copolymer solution, which reflects the salt resistance of the copolymer solution. In the mineralized water, as the apparent viscosity of the polymer solution decreased, the salt resistance increased. Clearly, as the apparent viscosity increases, the salt resistance of the polymer improves.

Figure 9 shows the relationship between *M* and the apparent viscosity for different UFPAM concentrations. It is obvious that lower UFPAM concentrations do not show salt resistance. However, salt resistance began to appear near to or above the CAC. The apparent viscosity of the 0.50 g dL^{-1} UFPAM solution was 478.8 mPa s in mineralized water (*M*= 29,621 mg/L) and 402.1 mPa s in a pure water solution, representing a difference of almost 20 %.

The degree of mineralization had an obvious effect on the self-assembly behavior according to the above results. The probability of association among the nonpolar hydrophobic groups in FA tended to increase due to the enhanced solution polarity in solutions with relatively low degrees of mineralization; accordingly, there was a large increase in the number of physical crosslinks. However, when *M* was in the range $3–6\times10^4$ mg/L, the apparent viscosity of the UFPAM solution dropped sharply. This result can be attributed to the shielding effect of the negative charges present in AMPS, which in turn lead to a reduction in electrostatic

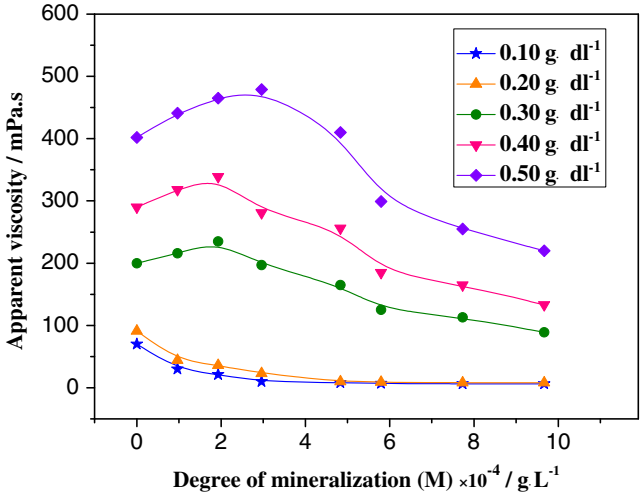

Fig. 9 Effect of *M* on the apparent viscosity for different UFPAM concentrations (shear rate: 7.6 s^{-1})

repulsion among polymer coils and among polymeric segments in the same coil. Consequently, there was less expansion of the polymer coils in solution. Also, the strong polarity led to weak hydrogen bonds. These factors both resulted in a relatively low hydrodynamic volume, synonymous with a lower viscosity. On the other hand, in solutions with a high degree of mineralization, the fluorinated hydrophobic groups in UFPAM formed associations, thus maintaining the apparent viscosity, which therefore did not fall sharply. In addition, the branching within the structure of UFPAM was markedly enhanced by the incorporation of AMPS, even when the strongly polar ionic groups in AMPS were shielded. These branched structures increased the steric hindrance, increasing the rigidity of the main chain and preventing polyacrylamide from hydrolyzing, which helped to maintain the apparent viscosity of the solution. We can therefore conclude that the self-assembly behavior of UFPAM in the mineralized water leads to good salt resistance properties.

Effect of temperature on the self-assembly behavior of UFPAM

The heat resistance of UFPAM was also reflected in the self-assembly behavior of UFPAM in aqueous solution at different temperatures. Figure 10 shows the effect of temperature on the apparent viscosity of UFPAM. The viscosity initially rose as the temperature was increased from 25 °C to 50 °C. The viscosity retention index (VRI, the ratio of the equilibrium viscosity to the initial viscosity) was used to represent the heat resistance performance. Based on calculations and analysis, the VRI of the 0.50 g dL^{-1} UFPAM solution reached 112.16 % at 30 °C and 89.29 % at 60 °C, respectively. This may be because the intramolecular associations were weakened to some extent by the increase in temperature, resulting in the expansion of the polymer coils. The stretching polymer coils were then more amenable to intermolecular association, resulting in an increase in the viscosity. However, when the temperature was increased beyond 50 °C, the thermal motions of the molecules intensified to a sufficient degree to weaken intermolecular associations. Hence, the apparent viscosity reduced. This indicates that applying a relatively high temperature could aid the self-assembly of UFPAM and thus improve its heat resistance.

Self-assembly behavior of UFPAM with low concentrations of ionic surfactants

A mixture of copolymer and surfactant is an important type of "soft material" system. The interaction of the surfactant with the copolymer not only affects the physical and chemical properties of the surfactant, but it also changes the conformation and shape of the polymer chain and the performance of the copolymer solution [32]. In addition, this kind of solution system has many unique properties due to the potential for static or hydrophobic interactions between the copolymer and the surfactant, which has always been a very interesting subject for researchers [33, 34].

The variations in the self-assembly behavior of the solution system when different ionic surfactants were added were investigated. Low concentrations of the two surfactants (i.e., far below their CMCs) were used in the investigation.

Figure 11a shows the effect of adding an anionic surfactant (sodium dodecyl sulfate, SDS) on the apparent viscosities of aqueous UFPAM solutions. When *c*(UFPAM)=0.30 g dL^{-1}, the apparent viscosity of the UFPAM solution increased as more SDS was added. The reason for this is that stable microdomains arising from intermolecular hydrophobic associations are not generated prior to reaching the CAC of

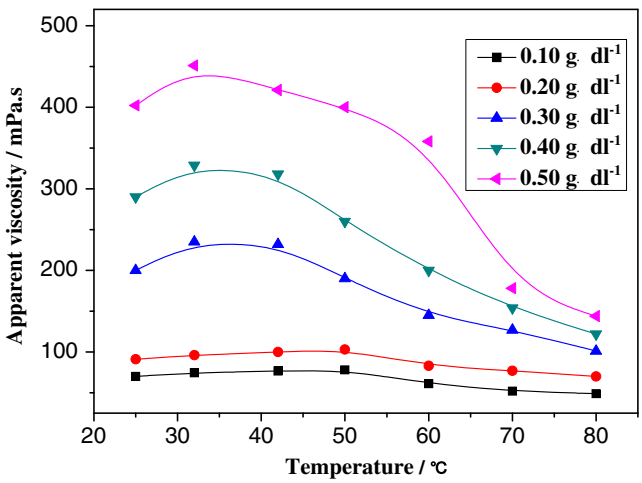

Fig. 10 Effect of temperature on the solution viscosity (shear rate: 7.6 s^{-1})

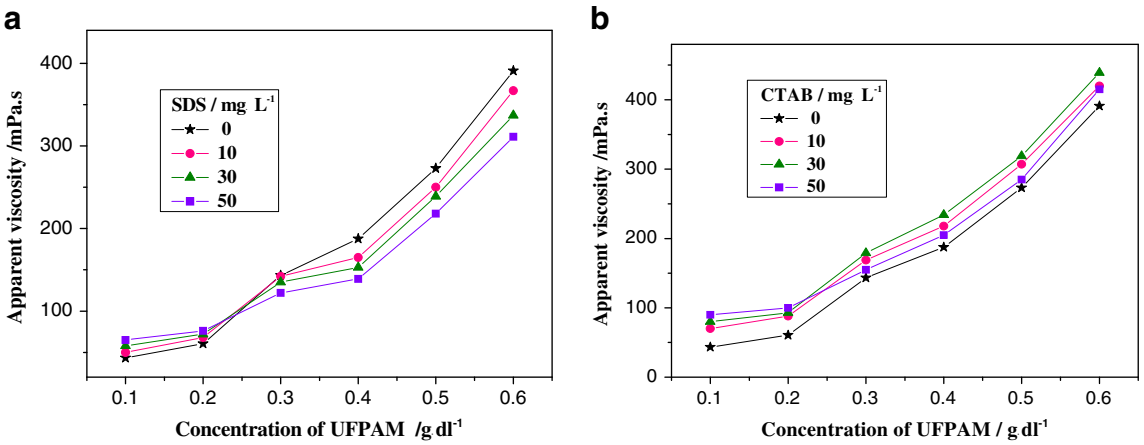

Fig. 11a–b Self-assembly behavior of UFPAM with ionic surfactants. **a** Effect of the UFPAM concentration on the apparent viscosity at different SDS concentrations. **b** Effect of the UFPAM concentration on the apparent viscosity at different CTAB concentrations

UFPAM; the hydrophobic groups of SDS are embedded in hydrophobic microdomains of the FA in the UFPAM, which reinforces the stability of these hydrophobic microdomains and thus enhances the hydrophobic association among macromolecules. However, when *c*(UFPAM) increases beyond the CAC, the apparent viscosity drops with increasing SDS content. At such high UFPAM concentrations, there are already stable hydrophobic microdomains in the UFPAM solution; adding SDS to it adversely affects the stability of these microstructures, altering the stable original hydrophobic associations and transforming the micelles from hydrophobic associations between macromolecules into "mixed micelles" comprising polymer macromolecules and SDS. Therefore, from a macroscopic point of view, the apparent viscosity drops. The micelles initially break up and then self-assemble.

Figure 11b shows the effect of adding a cationic surfactant (cetyltrimethyl ammonium bromide, CTAB) on the apparent viscosities of aqueous UFPAM solutions. As more CTAB is added to each solution, the apparent viscosity of the UFPAM solution rises. The reason for this may be that CTAB, with its cationic groups, combines with the anionic groups of the AMPS in the UFPAM molecules, leading to long-chain "comb-type" hydrophobic groups in the side chains of UFPAM. This increases the hydrophobicity of the UFHAM molecules and obviously enhances the intermolecular hydrophobic associations, leading to a sharp rise in the apparent viscosity of the aqueous solution [35]. However, when the concentration of UFPAM is near to or above the CAC of UFPAM, increasing the CTAB content beyond a certain level leads to a drop in the apparent viscosity. The reason for this is similar to the cause of the effect of SDS on the properties of UFPAM solutions (see above).

We can therefore conclude that different types of ionic surfactant in UFPAM solutions yield different self-assembly behaviors of this anionic fluorinated hydrophobically associating polyacrylamide. Also, we can speculate that these cationic and anionic surfactants will have the opposite effects to those described above when they are added to a cationic fluorinated hydrophobically associating polyacrylamide; however, further research will need to be carried out to verify this speculation.

Micelle aggregation number

Steady-state fluorescence quenching is a method that is commonly used to study the aggregation of amphiphilic copolymers, and can be used to study the micelle aggregation number *N* for the micelles generated between a surfactant and polymer. We therefore used this technique to investigate the micelles generated between SDS and UFPAM, and between CTAB and UFPAM. The concentration of pyrene employed in this study was 1.00×10^{-6}mol L^{-1}, and the concentration of quenching agent used was in the range 0–

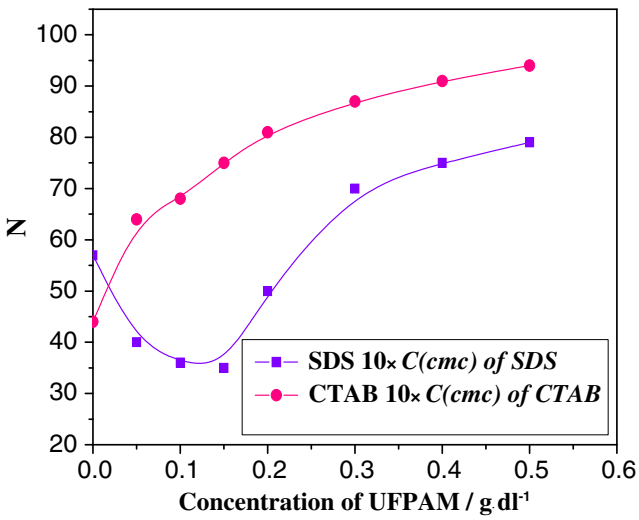

Fig. 12 Effect of *c*(UFPAM) on the micelle aggregation numbers *N* for two surfactant solutions

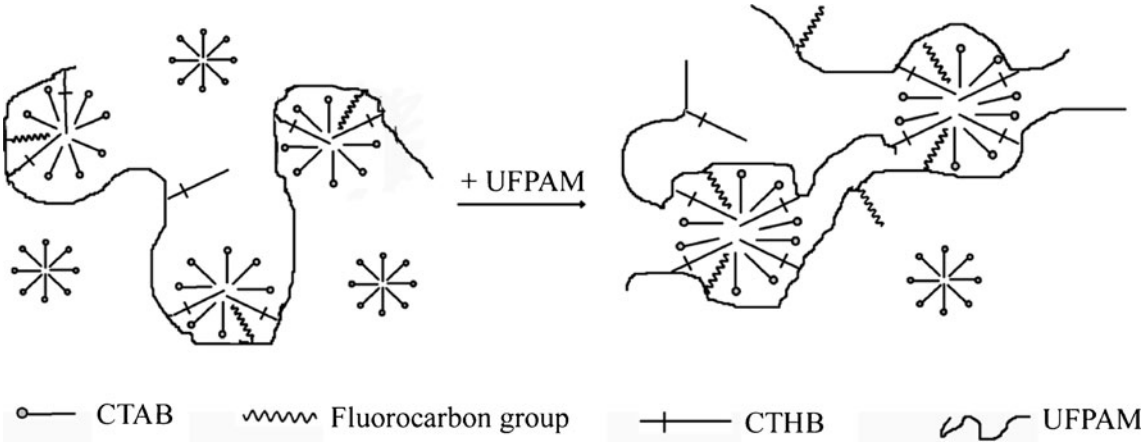

Scheme 1 Changes in the mixed micelles in CTAB solution with increasing *c*(UFPAM)

0.025 mmol L^{-1}. The concentrations of both surfactant solutions used were ten times their CMCs. The *N* values for both surfactants were calculated using Eq. 1. The experimental results of this study are shown in Fig. 12. The aggregation numbers *N* of the ionic surfactants changed markedly as UFPAM was added to the solution, although they varied in very different ways with increasing UFPAM concentration.

For the anionic surfactant SDS, the aggregation number *N* initially decreased but then increased with increasing *c* (UFPAM). The minimum value of *N* was about 35, which occurred at *c*(UFPAM)=0.15 g dL^{-1}. The reason for this behavior is that the hydrophobic groups of UFPAM interact with the micelles of SDS when UFPAM is added to the surfactant solution. This initially leads to the disassembly of the original micelles at low UFPAM concentrations, but as the amount of UFPAM increases, new "mixed micelles" are formed between the UFPAM and the SDS. Additionally, as the concentration of UFPAM increases, the total number of mixed micelles in the system increases, which decreases the *N* in each micelle. However, as the *c*(UFPAM) continues to increase, the number of hydrophobic groups FA in the system increases, which tend to aggregating mutually together within the "mixed micelles," as a result, the value of *N* increases. Therefore, the aggregation number *N* initially decreases to a minimum and then increases.

For the cationic surfactant CTAB, the aggregation number *N* increases with increasing *c*(UFPAM)—there is no minimum. This may be because the CTAB can combine with the anionic groups in the AMPS in the copolymer molecules through ionic bonding, leading to the formation of long-chain "comb-type" hydrophobic groups (CTHB) in the side chains of UFPAM, which increases the hydrophobicity of UFPAM.

As *c*(UFPAM) increases, the number of macromolecules and the number of hydrophobic groups within the FA in the copolymer both increase, meaning that the macromolecules exhibit a strong tendency for self-association via intermolecular interactions among their hydrophobic side chains. However, there are three kinds of hydrophobic groups in the system: fluorocarbon groups, CTHB, and CTAB. These groups repel each other to a certain degree due to the oleophobicity of the fluorocarbon chains. Also, the lengths of the three kinds of hydrophobic groups are different, leading to disorder and looseness within the mixed micelles, and increasing the Gibbs free energy of the solution system. Therefore, the mixed micelles that are formed lack thermodynamic stability, which prompts the CTAB micelles to split and add more CTAB to the mixed micelles in order to achieve thermodynamic stability. This results in large mixed micelles and thus an enhanced aggregation number *N* (Scheme 1).

Conclusions

(1) UFPAM was successfully prepared from AM, AMPS, and FA using an ultrasound-assisted polymerization method. The CAC of aqueous UFPAM was determined as 0.31 g dL^{-1} based on rheological data. The results of investigations indicate that aqueous UFPAM is a pseudoplastic fluid, and that the self-assembly behavior of the UFPAM clearly influences the parameters G', G'', and d^*. When *c*(UFPAM) was 0.40 g dL^{-1}, the relaxation time τ_c and d^* reached 5.5 s and 2,270 nm, respectively.

(2) The self-assembly behavior of UFPAM in mineralized water led to good salt resistance properties. The apparent viscosity of a 0.50 g dL^{-1} UFPAM solution in mineralized water (*M*=29,621 mg/L) was almost 20 % higher than its apparent viscosity in pure water. At same time, applying a relatively high temperature improved the heat resistance of UFPAM. The VRI of 0.50 g dL^{-1} reached 112.16 % at 30 °C and 89.29 % at 60 °C, respectively.

(3) Low concentrations of the anionic surfactant SDS enhanced the self-assembly behavior of UFPAM solutions below the CAC, but hindered this behavior above the CAC. On the other hand, the addition of

low concentrations of the cationic surfactant CTAB always enhanced the self-assembly of UFPAM, whatever its concentration, leading to a continuous increase in the apparent viscosity with UFPAM concentration. This thickening effect of UFPAM addition decreased in strength with increasing c(CTAB).

(4) The micelle aggregation number N for a solution of the anionic surfactant SDS initially decreased but then increased with the addition of UFPAM, leading to a minimum value of N of about 35, which occurred at c(UFPAM)=0.15 g dL^{-1}. On the other hand, the aggregation number N for a solution of the cationic surfactant CTAB continuously increased with the addition of UFPAM.

Acknowledgments We would like to express our great thanks to the Natural Science Foundation of China (50973057) and the Natural Science Foundation of Shaanxi Province (2012JQ2004, 2012JQ2005) as well as the Major Scientific and Technological Innovation Foundation of Shaanxi Province (2011ZKC04-3).

References

1. Zhang Y, Wu F, Li M, Wang E (2005) Novel approach to synthesizing hydrophobically associating copolymer using template copolymerization: the synthesis and behaviors of acrylamide and 4-(ω-propenoyloxyethoxy) benzoic acid copolymer. J Phys Chem B 47:22250–22255
2. Cram SL, Brown HR, Spinks GM, Hourdet D, Creton C (2005) Hydrophobically modified dimethylacrylamide synthesis and rheological behavior. Macromolecules 7:2981–2989
3. Charpentier VD, Merle L, Mocanu G, Picton L, Muller G (2005) Rheological properties of hydrophobically modified carboxymethylcelluloses. Carbohydr Polymer 60:87–94
4. Leibler L, Rubinstein M, Colby R (1991) Dynamics of reversible networks. Macromolecules 24:4701–4707
5. Goodwin JW, Hugues RW (1997) Particle interactions and dispersion rheology. ACS Symp Ser 663:94–125
6. Volpert E, Selb J, Candau F, Green N, Argillier JF, Audibert A (1998) Adsorption of hydrophobically associating polyacrylamides on clay. Langmuir 7:1870–1879
7. Zhu Z, Jian O, Paillet S, Desbrières J, Grassi B (2007) Hydrophobically modified associating polyacrylamide (HAPAM) synthesized by micellar copolymerization at high monomer concentration. Eur Polym J 3:824–834
8. Jimenez RE, Selb J, Candau F (2000) Effect of surfactant on the viscoelastic behavior of semidilute solutions of multisticker associating polyacrylamides. Langmuir 23:8611–8621
9. Sabhapondit A, Borthakur A, Haque I (2003) Characterization of acrylamide polymers for enhanced oil recovery. J Appl Polym Sci 87:1869–1878
10. Ma J, Liang B, Cui P, Dai H, Huang R (2003) Dilute solution properties of hydrophobically associating polyacrylamide: fitted by different equations. Polymer 44:1281–1286
11. Ye L, Huang RH (1999) Study of P(AM-NVP-DMDA) hydrophobically associating water-soluble terpolymer. J Appl Polym Sci 74:211–217
12. Zhang Y, Da A, Butler GB, Hogen-Esch T (1992) A fluorine-containing hydrophobically associating polymer. I. Synthesis and solution properties of copolymers of acrylamide and fluorine-containing acrylates or methacrylates. J Polym Sci A Polym Chem 30(7):1383–1391
13. Candau F, Selb J (1999) Hydrophobically-modified polyacrylamides prepared by micellar polymerization. Adv Colloid Interface 79:149–172
14. Gao BJ, Guo HP, Wang J, Zhang Y (2008) Preparation of hydrophobic association polyacrylamide in a new micellar copolymerization system and its hydrophobically associative property. Macromolecules 8:2890–2897
15. Xia HS, Wang Q, Qiu GH (2003) Polymer-encapsulated carbon nanotubes prepared through ultrasonically initiated in situ emulsion polymerization. Chem Mater 15(20):3879–3886
16. Okudaira G, Kamogawa K, Sakai T, Sakai H, Abe M (2003) Suspension polymerization of styrene monomer without emulsifier and initiator. J Oleo Sci 3:167–170
17. Song H, Zhang SF, Ma XC, Wang DZ, Yang JZ (2007) Synthesis and application of starch-graft-poly(AM-co-AMPS) by using a complex initiation system of CS-APS. Carbohydr Polymer 69:189–195
18. Blagodatskikh IV, Vasil'eva OV, Ivanova EM, Bykov SV, Churochkina NA, Pryakhina TA, Smirnov VA, Philippova OE, Khokhlov AR (2004) New approach to the molecular characterization of hydrophobically modified polyacrylamide. Polymer 45:5897–5904
19. Sharma KS, Hassan PA, Rakshit AK (2006) Self aggregation of binary surfactant mixtures of a cationic dimeric (gemini) surfactant with nonionic surfactants in aqueous medium. Colloids Surf A 289:17–24
20. Pretsch E, Buhlmann P, Affolter C (2000) Structure determination of organic compounds: tables of spectral data. Springer, Berlin, pp 1–400
21. Christian S, Dieter N, Harald S, Josef H (2001) Concepts in the NMR structural analysis of perfluoroalkyl groups: characterization of the bis(n-perfluoroalkyl)zinc compounds: Zn(n-C_mF_{2m+1})$_2$·2THF (m = 4, 6, 7, 8) and Zn(n-C_6F_{13})$_2$·2CH_3CN. J Fluor Chem 107(1):159–169
22. Iliuta I, Larachi F (2002) Hydrodynamics of power-law fuids in trickle-flow reactors: mechanistic model, experimental verification and simulations. Chem Eng Sci 57:1931–1942
23. Yu YM, Gao BJ, Wang RX (2005) Synthesis of surface active monomer NaAMC14S and research of its micellar behavior. Chin J Colloid Polymer 4:26–28
24. Beghein N, Rouxhet L, Dinguizli M, Brewster M, Ariën A, Préat V, Habib J, Gallez B (2007) Characterization of self-assembling copolymers in aqueous solutions using electron paramagnetic resonance and fluorescence spectroscopy. J Contr Release 117 (2):196–203
25. Ren BY, Gao YM, Liu X, Tong Z (2006) Aggregates of alginates binding with surfactants of single and twin alkyl chains in aqueous solutions: fluorescence and dynamic light scattering studies. Carbohydr Polym 66(2):266–273
26. Shashkina YA, Zaroslov YD, Smirnov VA, Philippova O, Khokhlov A, Pryakhina T, Churochkina A (2003) Hydrophobic aggregation in aqueous solutions of hydrophobically modified polyacrylamide in the vicinity of overlap concentration. Polymer 44(8):2289–2293
27. Nga WK, Tama KC, Jenkins RD (2001) Rheological properties of methacrylic acid/ethyl acrylate co-polymer:comparison between an unmodified and hydrophobically modified system. Polymer 42:249–259
28. Volpert E, Selb J, Candau F (1998) Associating behaviour of polyacrylamides hydrophobically modified with dihexylacrylamide. Polymer 39:1025–1033
29. Klucker R, Munch JP, Schosseler F (1997) Combined static and dynamic light scattering study of associating random block copolymers in solution. Macromolecules 30:3839–3848
30. Boger DV (1977) Demonstration of upper and lower Newtonian fluid behaviour in a pseudoplastic fluid. Nature 265:126–128

31. Rosentrater KA, Flores RA (1997) Physical and rheological properties of slaughterhouse swine blood and blood conponents. Trans ASABE 40(3):683–689
32. Goddard ED (2002) Polymer/surfactant interaction: interfacial aspects. J Colloid Interface Sci 256:228–235
33. Sastry NV, Hoffmann H (2004) Interaction of amphiphilic block copolymer micelles with surfactants. Colloids Surf A 250:247–261
34. Puspendu D, Somasundaran P (2005) Interactions of hydrophobically modified polyelectrolytes with nonionic surfactants. Langmuir 21:3950–3956
35. Smith GL, McCormick CL (2001) Water-soluble polymers. 79. Interaction of microblocky twin-tailed acrylamido terpolymers with anionic, cationic, and nonionic surfactants. Langmuir 17:1719–1725